

Control of Photovoltaic Water Pumping System

Chafia Serir
serirch@yahoo.fr

Department of Electrical Engineering, University of Bejaia
Laboratory LTII,
Bejaia, Algeria

Djamila Rekioua
dja_rekioua@yahoo.fr

Department of Electrical Engineering, University of Bejaia
Laboratory LTII,
Bejaia, Algeria

Abstract—Due to the continuous decrease of the solar cells cost, photovoltaic energy is used in different applications. The most important one is the water pumping system powered by photovoltaic generators. These systems can work with or without storage battery. With the increased use of this application, more attention has been paid to their optimum utilization. Many methods have been developed to determine the maximum power point (MPP). In this paper, to control the DC bus voltage, we apply field oriented control (FOC) strategy to induction motor (IM) supply by a photovoltaic (PV) system. And to maximize the efficiency of the proposed PV pumping system, we use the fuzzy logic controller (FLC) and the classical Perturb and Observ (P&O). Different tests have been carried to prove the effectiveness of the proposed control system.

Keywords- Pumping Photovoltaic system, Fiel oriented contorl, MPPT, Fuzzy logic controle, Perturb and Observ.

I. INTRODUCTION

The photovoltaic array has a unique operating point (MPP) that can supply maximum power to the load. The locus of this point has a non-linear variation with solar irradiation and temperature. Therefore, to maximize the efficiency of the photovoltaic energy system, it is necessary to track the maximum power point of the PV array. Many methods and controllers have been widely developed and implemented to track the maximum power point (MPP) [2-6]. Most control schemes use the Perturb and Observ (P&O) method which is based on iterative algorithms to track continuously the MPP, because it is easy to implement [2,3] but the oscillation problem is unavoidable. In many references the effectiveness of a fuzzy logic controller is shown [2-5] compared to the (P&O) method. It improves control robustness and this control gives robust performance under parameters and load variation. Several authors present much attention to the study of the dynamic performance of the photovoltaic pumping systems. A. Terki and al [7] presented an analysis of the dynamic performance of a permanent magnet brushless DC motor controlled through a hysteresis current loop. Betka [8] presented the performance optimization of an asynchronous motor associated at a PV generator. Recently, vectorial command of induction motor pumping system supplied by photovoltaic generator was studied by Makhoulf and al [9]. In H. Hadi [10], the photovoltaic pumping system with battery is proposed to reduce the overheating of the motor temperature and increase the efficiency. The battery is installed as the storage of the surplus energy and backup energy.

In this paper, we present a PV pumping water which includes photovoltaic array generator, DC/DC converter, DC/AC converter and induction motor coupled to a centrifugal pump. The FLC controller is applied to ensure a a maximum operating of the photovoltaic array. And to improve the FLC controller, we make a comparison with the classical MPPT, the Perturb and Observ (P&O). Obtained results are presented.

II. PROPOSED SYSTEM DESCRIPTION

The proposed studied system is shown in Fig.1. It consists of a photovoltaic-pumped system, composed of a PV generator, DC-AC converter, a field oriented controlled induction motor and centrifugal pump.

A. Photovoltaic generator model

This model is characterized by a very simple resolution. It requires only four parameters namely I_{sc} , V_{oc} , V_{mp} and I_{mp} . The I_{pv} - V_{pv} characteristic of this model is illustrated as follows:

$$I_{pv} = I_{sc} \left\{ 1 - C_1 \left[\exp \left(\frac{V_{pv}}{C_2 \cdot V_{oc}} \right) - 1 \right] \right\} \quad (1)$$

With:

$$C_2 = \frac{\left(\frac{V_m}{V_{oc}} \right) - 1}{\ln \left(1 - \frac{I_m}{I_{sc}} \right)}$$

$$C_1 = \left(1 - \frac{I_m}{I_{sc}} \right) \exp \left(- \frac{V_m}{C_2 \cdot V_{oc}} \right)$$

We make validation through the following experimental bench (Fig.3.)



Fig.3. Experimental PV bench,

Specifically, if the power panel is increased due to the disturbance, the following disturbance will be made in the same direction. And if the power decreases, the new perturbation is made in the opposite direction. The advantages of this method can be summarized as follows: knowledge of the characteristics of the photovoltaic generator is not required, it is relatively simple. Nevertheless, in steady state, the operating point oscillates around the MPP, which causes energy losses. The MPPT is necessary to draw the maximum amount of power from the PV module [8-11].

B.2. Fuzzy logic controller

Fuzzy logic controller is introducing to determine the operating point corresponding to maximum power for different insolation levels and temperature. In this case, inputs of the fuzzy logic controller are power variation (ΔP_{pv}) and voltage variation (ΔV_{pv}). The output is reference voltage variation ($\Delta V_{pv,ref}$). In order to converge towards the optimal point, rules are relatively simple to establish. These rules depend on the variations of power ΔP_{pv} and voltage ΔV_{pv} . In accordance with Table.3, if the power (P_{pv}) increased, the operating point should be increased as well. However, if the power (P_{pv}) decreased, the voltage ($V_{pv,ref}$) should do the same.

Table.2
Fuzzy rule table [27].

| $\Delta P_{pv} \backslash \Delta V_{pv}$ | BN | MN | SN | Z | SP | MP | BP |
|--|----|----|----|---|----|----|----|
| BN | BP | BP | MP | Z | MN | BN | BN |
| MN | BP | MP | SP | Z | SN | MN | BN |
| SN | MP | SP | SP | Z | SN | SN | MN |
| Z | BN | MN | SN | Z | SP | MP | BP |
| SP | MN | SN | SN | Z | SP | SP | MP |
| MP | BN | MN | SN | Z | SP | MP | BP |
| BP | BN | BN | MN | Z | MP | BP | BP |

From these linguistic rules, the MPPT algorithm contain measurement of variation of photovoltaic power ΔP_{pv} and variation of photovoltaic voltage ΔV_{pv} proposes a variation of the voltage reference $\Delta V_{pv,ref}$ according to eq.2.

$$\begin{cases} \Delta P_{pv} = P_{pv}(k) - P_{pv}(k-1) \\ \Delta V_{pv} = V_{pv}(k) - V_{pv}(k-1) \\ V_{pv-ref}(k) = V_{pv}(k-1) + \Delta V_{pv-ref}(k) \end{cases} \quad (2)$$

Where: $P_{pv}(k)$ and $V_{pv}(k)$ are the power and voltage of the photovoltaic generator at sampled times (k), and $V_{pv,ref}(k)$ the instant of reference voltage

C. Modeling subsystem pumping

Many different varieties of pumps are used with PV-pumping system. In our case, we use the model expresses the water flow output (Q) directly as a function of the electrical power input (P) to the motor-pump, for different total heads. A polynomial fit of the third order expresses the relationship between the flow rate and power input, as described by the following equation [6, 7]:

$$P(Q, h) = a(h)Q^3 + b(h)Q^2 + c(h)Q + d(h) \quad (3)$$

Where P is the electrical power input of the motor-pump, h is the total head and a(h), b(h), c(h), d(h) are the coefficients corresponding to the working total head.

With: a_i , b_i , and d_i constants which depend on the type of sub-solar pumping system.

The calculation of the instantaneous flow in terms of power is calculated using Newton-Raphson method. Thus at the k^{th} iteration, the flow Q is given by the following equation:

For $d - P_a(Q) > 0$:

$$Q_k = Q_{k-1} - \frac{F(Q_{k-1})}{F'(Q_{k-1})} \quad (4)$$

With:

$$F(Q_{k-1}) = aQ_{k-1}^3 + bQ_{k-1}^2 + cQ_{k-1} + d - P_a(Q_{k-1}) \quad (12)$$

$F'(Q_{k-1})$ is the derivative of the function $F(Q_{k-1})$

We use an induction motor which is modeled using voltage and flux equations referred in a general frame:

$$\begin{cases} V_{sd} = R_s I_{sd} + \frac{d\Phi_{sd}}{dt} \\ V_{sq} = R_s I_{sq} + \frac{d\Phi_{sq}}{dt} \end{cases} \quad (5)$$

Where: (I_{sd}, I_{sq}) , (V_{sd}, V_{sq}) and (Φ_{sd}, Φ_{sq}) are the (d,q) components of the stator current, voltage and flux, R_s is the stator resistance.

$$\begin{cases} 0 = V_{rd} = R_r I_{rd} + \frac{d\Phi_{rd}}{dt} + \frac{d\theta}{dt} \Phi_{rq} \\ 0 = V_{rq} = R_r I_{rq} + \frac{d\Phi_{rq}}{dt} - \frac{d\theta}{dt} \Phi_{rd} \end{cases} \quad (14)$$

Where: I_{rd} , I_{rq} are (d,q) rotor current, Φ_{rd} , Φ_{rq} are (d,q) rotor flux, R_r is the rotor resistance.

We obtain the follow mathematical model:

$$\begin{bmatrix} \frac{di_{ds}}{dt} \\ \frac{di_{qs}}{dt} \\ \frac{di_{dr}}{dt} \\ \frac{di_{qr}}{dt} \end{bmatrix} = \frac{1}{\sigma} \begin{bmatrix} -\frac{R_s}{L_s} & \frac{P \cdot \omega_r \cdot L_m^2}{L_s \cdot L_r} & \frac{L_m \cdot R_r}{L_s \cdot L_r} & \frac{P \cdot \omega_r \cdot L_m}{L_s} \\ -\frac{P \cdot \omega_r \cdot L_m^2}{L_s \cdot L_r} & -\frac{R_s}{L_s} & \frac{P \cdot \omega_r \cdot L_m}{L_s} & \frac{L_m \cdot R_r}{L_s \cdot L_r} \\ \frac{L_m \cdot R_s}{L_s \cdot L_r} & -\frac{P \cdot \omega_r \cdot L_m}{L_r} & -\frac{R_r}{L_r} & -P \cdot \omega_r \\ \frac{P \cdot \omega_r \cdot L_m}{L_r} & \frac{L_m \cdot R_s}{L_s \cdot L_r} & P \cdot \omega_r & -\frac{R_r}{L_r} \end{bmatrix} \begin{bmatrix} i_{ds} \\ i_{qs} \\ i_{dr} \\ i_{qr} \end{bmatrix} + \frac{1}{\sigma} \begin{bmatrix} \frac{1}{L_s} & 0 \\ 0 & \frac{1}{L_s} \\ -\frac{L_m}{L_s \cdot L_r} & 0 \\ 0 & -\frac{L_m}{L_s \cdot L_r} \end{bmatrix} \begin{bmatrix} v_{ds} \\ v_{qs} \end{bmatrix} \quad (6)$$

With: σ is the leakage coefficient

-The mechanical equation is given as:

$$T_{em} - T_{Load} = J \cdot \frac{d\omega_r}{dt} \quad (7)$$

With: ω_r is the AC motor velocity angular, J the inertia of the AC motor.

The electromagnetic torque can be written as:

$$T_{em} = P \cdot (\phi_{sd} i_{sq} - \phi_{sq} i_{sd}) \quad (8)$$

III. FIELD ORIENTED CONTROL

In our work, we choose the orientation of rotor flux such as:

$\Phi_{rd} = \Phi_r$ and $\Phi_{rq} = 0$. This means that the flux Φ_r is

aligned permanently along the d-axis. Finally, as the chosen frame implies $\Phi_{rq} = 0$, the expression of the electromagnetic torque becomes:

$$T_e = p \cdot \frac{M}{L_r} \cdot \Phi_r \cdot i_{sq} \quad (9)$$

The rotor flux as a function of the current i_{sd} and the rotor time constant $T_r = L_r/R_r$ is given by the following expression:

$$\Phi_r = \frac{M \cdot i_{sd}}{1 + T_r \cdot s} \quad (10)$$

Where: s represents the derivative operator.

The knowledge of ω_s , by using the internal angular relation

$\omega_s = \omega_r + p \cdot \Omega$ and the mechanical speed of the machine Ω is measured continuously; the speed of the rotor field is estimated by the following expression:

$$\omega_r = \frac{M \cdot i_{sq}}{T_r \cdot \Phi_r} \quad (11)$$

Then, ω_s can be written in the following way:

$$\omega_s = \frac{M \cdot i_{sq}}{T_r \cdot \Phi_r} + p \cdot \Omega \quad (12)$$

The output power P_{pv} from PV will be fed to induction motor pump relating with torque and speed can be shown in the following equation

$$T_{em} = K \cdot \omega^2 \quad (13)$$

The mechanical output power of induction motor pump is:

$$P_{mec} = K \cdot \omega^3 \quad (14)$$

where K is the Pump constant.

From energy theory ($P_{i,,} = P_{o,,} = P$,) the frequency angle is:

$$\omega = \sqrt[3]{\frac{P_{pv}}{K}} \quad (15)$$

The mechanical torque of induction motor pump can be written as:

$$T_{em} = \sqrt[3]{K \cdot P_{pv}^2} \quad (16)$$

IV. NUMERICAL SIMULATION

In order to prove the robustness of the proposed MPPT using FLC, we compare it with conventional MPPT using P&O algorithm in terms of tracking of the PPM at different tests conditions (High, medium and low irradiances).

We make error calculation of the power and voltage at steady state for the two MPPT methods (Table 3.). We use the following expressions:

$$\varepsilon_p (\%) = \left| \frac{P_{pv_{max, madele, \acute{e}lectrique}} - P_{pv_{max}}}{P_{pv_{max, madele, \acute{e}lectrique}}} \right| 100 \quad (17)$$

$$\varepsilon_v (\%) = \left| \frac{V_{pv_{max, madele, \acute{e}lectrique}} - V_{pv_{max}}}{V_{pv_{max, madele, \acute{e}lectrique}}} \right| 100 \quad (18)$$

The efficiency can be calculated by:

$$\eta (\%) = \frac{P_{pv_{max}}}{P_{max}} 100 \quad (19)$$

With: $V_{pv_{max}}$ and $P_{pv_{max}}$ are voltage and power obtained with MPPT.

Table.3.

Error calculation for the two method s under different conditions

| Tests conditions | MPPT | $\varepsilon_p (\%)$ | $\varepsilon_v (\%)$ |
|--|----------------|----------------------|----------------------|
| <u>High irradiance</u> E=850 W/m ² T=35°C | P&O | 0.630 | 1.220 |
| | FLC | 0.190 | 0.090 |
| <u>Medium irradiance</u> E=500 W/m ² T=28°C | P&O | 1.740 | 1.100 |
| | FLC | 1.060 | 0.060 |
| <u>Low irradiance</u> E=350 W/m ² T=17°C | P&O | 0.570 | 0.820 |
| | FLC | 0.280 | 0.330 |

Table.4.

Efficiency of two methods under STC test conditions

| STC Test condition | MPPT | $\eta (\%)$ |
|-----------------------------------|------------|-------------|
| E=1000 W/m ² T=25°C | PO | 99.409 |
| | FLC | 99.822 |

V. APPLICATION

We make a sizing of the various components of the studied system which consists of a water tank of 70 m³ to satisfy the domestic needs of a family. The dynamic level head is about 12m and the nominal flow rate is of 21m³/h. Table5. summarizes the obtained results of the sizing system.

Table5.

Sizing pumping system

| Symbols | Expressions | Results |
|---------------|--|-----------------------|
| P_{hyd} | $P_{hyd} = \rho \cdot g \cdot HMTQ_n$ | 680W |
| P_{mec} | $P_{mec} = \frac{P_{hyd}}{\eta_{pump}}$ | 1240W |
| P_{elec} | $P_{elec} = \frac{P_{mec}}{\eta_{mec}}$ | 1470W |
| P_d | $P_d = \frac{P_{elec}}{\eta_{inv}}$ | 1550W |
| τ_d | $\tau_d = \frac{V}{Q_n}$ | 3.33hours |
| E_c | $E_c = \tau_d \cdot P_d$ | 5.16kWh/ day |
| P_g | $P_g = \frac{E_c}{\tau_p(l-\sum series)}$ | 1.94kW |
| N_{pv} | $N_{pv} \geq \frac{P_{pv_{max}}}{P_{max t}}$ | $N_{pv} = 18$ pannels |
| N_s | $N_{paralel} = \frac{I_m}{I_{opt}}$ | $N_s = 6$ pannels |
| $N_{paralel}$ | | $N_{paralel} = 3$ |

We obtain the following scheme (fig.5) with the different results:

$$U_{GPV} = N_{p.series} * I_{pv} = 6 * 35 = 210V$$

$$I_{GPV} = N_{braches} * I_{pv} = 3 * 3.14 = 9.42 A$$

$$P_{PV} = U_{GPV} * I_{GPV} = 210 * 9.42 = 1.978 kW$$

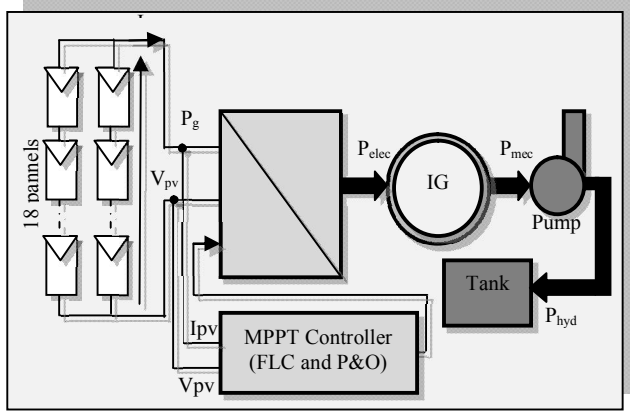


Fig. 5. Diagram power for the studied system

The induction machine parameters are given in Table 6

TABLE6.

Induction machine parameters

| | |
|---------------------------|------------------|
| Nominal power P_N | 1.5 (KW) |
| Nominal current I_{sn} | 5.2/3 (A) |
| Nominal voltage | 220/380 (V) |
| Frequency f | 50 (Hz) |
| Number of poles pairs p | 2 |
| Rated speed N_n | $N=1460$ (tr/mn) |

We make error calculation of the flow pump at steady state for the two MPPT methods (Table 5.). We use the following expressions:

$$\varepsilon_Q (\%) = \left| \frac{q_{v(désiré)} - Q_{mppt}}{q_{v(désiré)}} \right| 100 \quad (20)$$

And we calculate the pumped efficiency by:

$$\eta (\%) = \frac{P_h}{P_{mec}} 100 \quad (21)$$

We can remark, that MPPT strategies improve the pumping system compared to a direct coupling. The FLC gives us a fast response compared to P&O method which requires much time to track the Maximum Power Point (MPP).

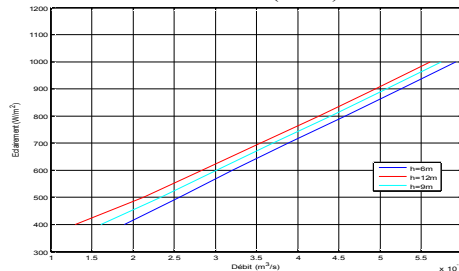


Fig.6 Water Flow for different heads

Table 7.
Comparison results with and without MPPT

| Strategies | Response time(s) | Pump flow Q_{MPPT} (m³/s) | Error pump flow ε_Q (%) | Pump Efficiency η (%) |
|-----------------|------------------|-----------------------------|-------------------------------------|----------------------------|
| FLC | 0.0178 | $5.613 \cdot 10^{-3}$ | 3.22 | 53.29 |
| P&O | 0.0552 | $5.298 \cdot 10^{-3}$ | 8.65 | 50.30 |
| Direct coupling | 0.273 | $4.600 \cdot 10^{-3}$ | 20.69 | 43.67 |

A vector control based on FLC of the induction motor, with optimization is used. Simulation results are carried out under variation of environmental conditions to verify the ability of the photovoltaic pumping system to give desired water flow in accordance to the user needs.

The reference speed is calculated from a reference power which is function on the water flow. The reference power is obtained from the available maximum photovoltaic power and the batteries which compensate the power deficit to provide a continuous delivery of energy to the motor pump. Simulation results using the vector control strategy are given. The flux and V_{dref} reference values are applied ($\Phi_{d-ref} = 0.7Wb$; $V_{dref} = 465V$). The control strategy is tested through the variations of insolation. The solar radiation varies up from 500 to 1000W/m² (fig.7.).

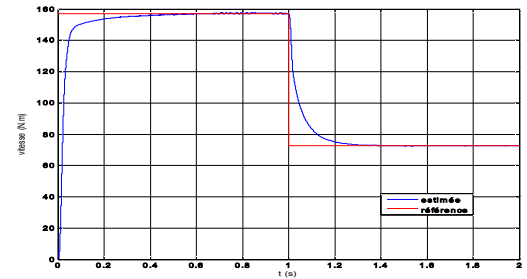


Fig.7 Reference Ω_{ref} and estimated Ω_{est} speed

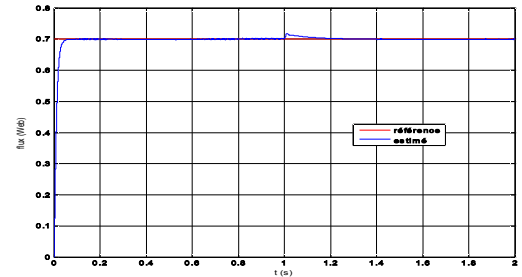


Fig.8 Rotor flux Φ_{rd} for (1000W/m² and 500W/m²)

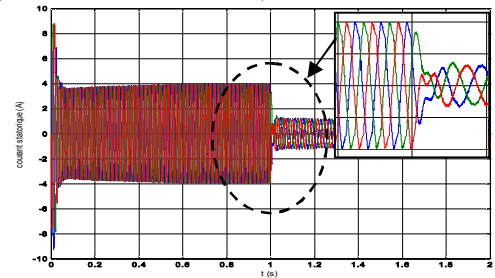


Fig.9 Stator currents for (1000W/m² and 500W/m²)

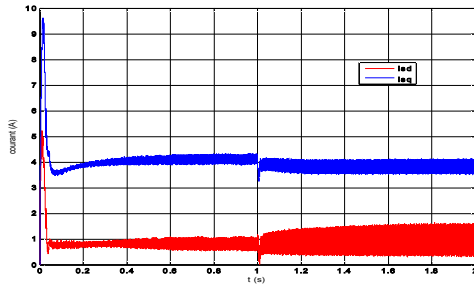


Fig.10 Currents waveforms Id,iq

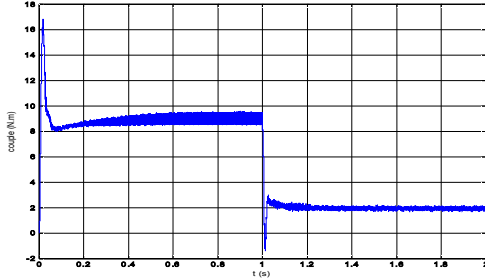


Fig.11 Electromagnetic torque

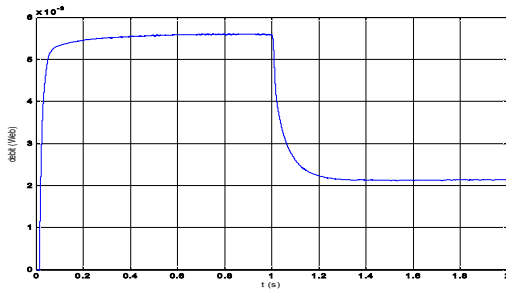


Fig.12 Water Flow

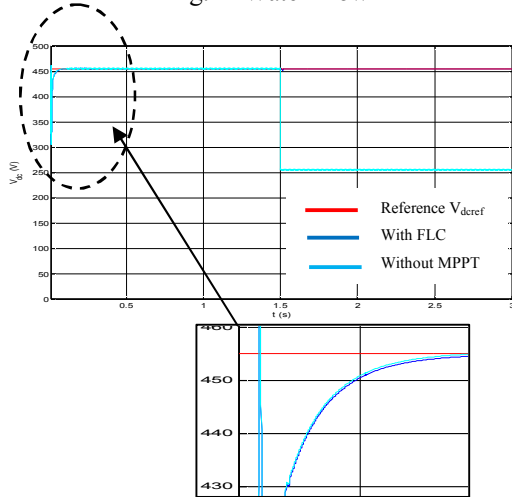


Fig.13. DC bus voltage

The FLC measures instantaneously PV voltage and current variations and determines quickly the optimal increment required to have the operating voltage for tracking the MPP even when the operating environmental conditions change rapidly. Fig. 10 shows the DC voltage waveform in the output of the DC converter. We note that the DC bus voltage kept constant and follows its reference V_{dcref} whatever insolation variations.

VI. CONCLUSION

In this paper, we have applied two MPPT methods (P&O, and FLC) to a photovoltaic pumping system with field oriented control (FOC). An application is made to satisfy water needs of a family. The simulation results show that the control with FLC method is more efficient in terms of stability, precision and speed to reach the maximum power point

VII. REFERENCES

- [1] Chenni, R. Zarour L., Bouzid A. and Kerbach T., "Comparative study of photovoltaic pumping systems using a permanent magnet synchronous motor (PMSM) and an asynchronous motor (ASM) ", *Rev. Energ. Ren.* vol. 9 , pp.17 – 28, 2006,
- [2] Lalouni S, Idjdarene K, Rekioua D, "Vector Control based on fuzzy logic controller of Induction Motor for Photovoltaic Pumping System", in Proc. IREC 2012, Tunis, 20-22, 2012, pp:1-6
- [3] Salas V., Olias E., Barrado A., Lazaro A., " Review of the Maximum Power Point Tracking Algorithms for Stand-Alone Photovoltaic Systems", *Solar Energy Materials & Solar Cells*, vol. 90, no.11, pp.1555-1578, 2006.
- [4] Lalouni S, Rekioua D, Rekioua T, Matagne E, "Fuzzy logic control of stand-alone photovoltaic system with battery storage", *Journal of Power Sources*, vol.193, no.2, pp. 899–907, 2009.
- [5] [Rekioua D., Bensmail S., Bettar N., Development of hybrid photovoltaic-fuel cell system for stand-alone application](#), (2014) *International Journal of Hydrogen Energy*, 39 (3) , pp. 1604-1611.
- [6] Patcharaprakiti N., Premrudeepreechacharn S., Sriuthaisiriwong Y, "Maximum power point tracking using adaptive fuzzy logic control for grid connected photovoltaic system". *Renewable Energy*, vol. 30, no.11, 2005, pp.1771-1788
- [7] Terki A., Moussi A., Betka A., Terki N., "An improved efficiency of fuzzy logic control of PMBLDC for PV pumping system", *Applied Mathematical Modelling*, Vol.36, no.3, pp. 934–944, 2012.
- [8] Betka A. and Moussi A., "Performance Optimization of a Photovoltaic Induction Motor Pumping System", *Renewable Energy*, vol. 29, pp. 2167 – 2181, 2004.
- [9] Makhoulouf M., Messai F., Benalla H., "vectorial command of induction motor pumping system supplied by a photovoltaic generator", *journal of electrical engineering*, vol. 62, no.1, pp: 3–10, 2011.
- [10] Rekioua D, Matagne E., *Optimisation of Photovoltaic Power Systems: Modelization, Simulation and Control*, Springer 2012.
- [11] [Rekioua D., Achour A.Y., Rekiouaa T., Tracking power photovoltaic system with sliding mode control strategy](#), (2013) *Energy Procedia*, 36 , pp. 219-230.